In-plane current-induced magnetization reversal of Pd/CoZr/MgO magnetic multilayers

Jing Liu(刘婧), Caiyin You(游才印)†, Li Ma(马丽), Yun Li(李云), Ling Ma(马凌), and Na Tian(田娜)

School of Materials Science and Engineering, Xi'an University of Technology, Xi'an 710048, *China*

(Received 30 June 2022; revised manuscript received 7 August 2022; accepted manuscript online 12 August 2022)

High critical current density ($> 10^6$ A/cm^2) is one of major obstacles to realize practical applications of the current-driven magnetization reversal devices. In this work, we successfully prepared Pd/CoZr(3.5 nm)/MgO thin films with large perpendicular magnetic anisotropy and demonstrated a way of reducing the critical current density with a low out-of-plane magnetic field in the Pd/CoZr/MgO stack. Under the assistance of an out-of-plane magnetic field, the magnetization can be fully reversed with a current density of about 10^4 A/cm^2. The magnetization reversal is attributed to the combined effect of the out-of-plane magnetic field and the current-induced spin-orbital torque. It is found that the current-driven magnetization reversal is highly relevant to the temperature owing to the varied spin-orbital torque, and the current-driven magnetization reversal will be more efficient in low-temperature range, while the magnetic field is helpful for the magnetization reversal in high-temperature range.

Keywords: critical current density, magnetization reversal, perpendicular magnetization, hybrid driving

PACS: 75.70.Cn, 75.47.–m, 75.70.Tj **DOI:** 10.1088/1674-1056/ac891d

1. Introduction

Magnetic random access memories (MRAMs) have attracted much attention due to their characteristics of high memory storage capacity, relatively low cost and stable information storage. In 1996, Berger and Slonczewski proposed that spontaneous magnetization precession could be driven or magnetic moment could be reversed under a certain critical current density.[1,2] It is theoretically investigated that the magnetic moment can be directly reversed through an electric current by spin-transfer torques (STTs) or spin-orbital torques (SOTs). In the current-driven cases, the energy consumption is much lower than the case of being driven by a magnetic field owing to the much lower current density. So far, the current-induced magnetization reversal through STTs and SOTs is widely investigated.[3,4] One of major purposes is of reducing the critical current density required to drive the magnetic moment reversal by improving the efficiency of the SOTs. The heavy metals with opposite signs of spin Hall angles are combined and used in the heterojunction to enhance the SOT.[5] The spin mixing conductance was improved by inserting a weak spin-orbital coupling material at the interface to enhance the spin transfer efficiency.[6] The SOT efficiency can also be enhanced by alloying Ni with Pt, which is favorable for lowering the critical switching current.[7] However, the critical current density of driving the magnetization reversal is still higher than 10^6 A/cm^2.[8]

On the other hand, the heavy metal/ferromagnetic metal (HM/FM) bilayer structure with perpendicular magnetic anisotropy (PMA) exhibits potentially high efficiency of the current-driven magnetization switching.[9–11] The orbital hybridization between Co 3d and O 2p is also helpful for getting the PMA.[12] CoZr possesses the merits of the high magnetocrystalline anisotropy, good corrosion resistance and radiation resistance,[13] potentially presenting good hard magnetic properties and multi-mode resonance frequencies.[14–16] However, there are few studies on perpendicular magnetic anisotropy and current-driven magnetization reversal of CoZr-based alloys although these alloys could be potential ferromagnetic candidates in the spintronic devices.

In view of the development of the hybrid car and heat-assisted recording, we may also develop a hybrid driving mode for magnetization reversal. In fact, it was demonstrated that an in-plane current could induce effective magnetic field to assist the magnetization reversal and domain wall motion in Pt/Co/Pt.[17,18] In this work, we successfully fabricated the perpendicular-magnetically anisotropic Pd/CoZr/MgO magnetic films. The in-plane current is applied to induce the SOT. Under an assistance of the out-of-plane magnetic field, the critical current density can be significantly reduced. The dependence of current-driven magnetization reversal on temperature is also analyzed through measuring the variations of Hall resistance at different temperatures.

2. Experimental

A series of films were deposited on Si/SiO$_2$ substrates by a magnetron sputtering technique at room temperature. The background vacuum was lower than 4×10^{-5} Pa. The stacks of films were prepared as follows: Si/Ta (6 nm)/Pd (1.8 nm)/CoZr (t nm)/MgO (1.5 nm)/Pd (1.5 nm) (t = 3.0–4.0) (hereinafter refer to Pd/CoZr (t nm)/MgO, and the top Pd

†Corresponding author. E-mail: caiyinyou@xaut.edu.cn

© 2022 Chinese Physical Society and IOP Publishing Ltd

layer was capped as a protective layer). The purity of $Co_{11}Zr_2$ target was better than 99.95%. The metal Ta layer and Pd layer were deposited under Ar pressure of 0.8 Pa with direct-current (DC) power of 50 W and 25 W, respectively. The ferromagnetic CoZr layer was deposited under Ar pressure of 1 Pa with DC power of 35 W. The MgO layer was deposited under Ar pressure of 0.8 Pa (10% oxygen) with radio frequency (RF) power of 150 W. The films were all annealed at temperature of 325 °C for 30 min under a vacuum below 10^{-5} Pa. The magnetic properties of the films were measured by the vibrating sample magnetometer (VSM: Lakeshore 7404). The Hall resistance of the magnetic multilayer films was measured (East Changing Technologies, China, ET9000) with a sample size of 6.5 mm long and 1 mm wide.

3. Results and discussion

Figure 1 shows the in-plane and out-of-plane hysteresis loops of Pd/CoZr (t nm)/MgO films with different thicknesses of ferromagnetic layers. As is shown, all films exhibit a feature of PMA. With increasing the thickness of the ferromagnetic layer, the Pd/CoZr (3.5 nm)/MgO film has a larger remanence ratio around 0.96. The PMA can be induced by the interfacial anisotropy, which usually requires a very thin magnetic layer.[19] However, it is well known that the Gilbert damping coefficient is related to the ferromagnetic layer thickness.[20] Thick ferromagnetic layer is helpful for achieving a low Gilbert damping coefficient, which is useful for realizing a low current density of magnetic reversal.[21] Here, PMA can be achieved in a relatively thick CoZr layer, and the effective anisotropy constant $K_{\rm eff} = 6.595 \times 10^5$ erg/cm^3 ($t_{\rm CoZr} =$ 3.5 nm), which would be very promising for development of advanced MRAMs.

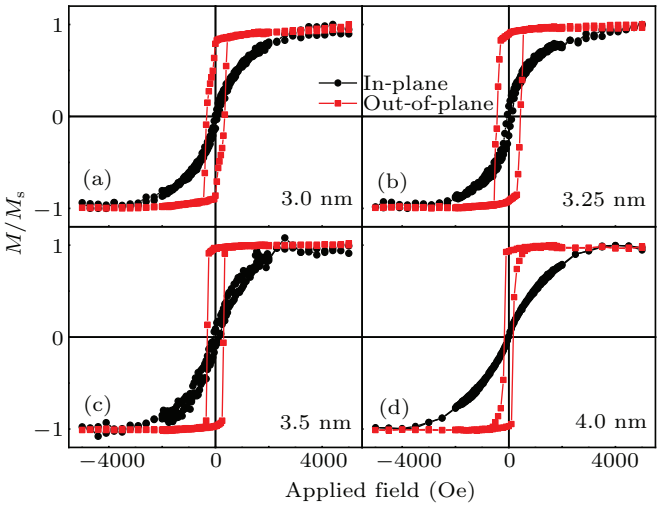


Fig. 1. The M–H loop of Pd/CoZr (t nm)/MgO film annealed: (a) 3.0 nm, (b) 3.25 nm, (c) 3.5 nm, (d) 4.0 nm.

Theoretically, thin films with PMA would be helpful for reducing critical current density. Figure 1 gives that the stack with 3.5 nm CoZr ferromagnetic layers presents the strongest PMA. Thus, the Pd/CoZr (3.5 nm)/MgO multilayer was selected to study the current-driven magnetization reversal. It is known that Hall resistance can reflect the magnetic moment orientation. The illustration in Fig. 2(a) shows a loop of Hall resistance measured at 294 K, indicating the good PMA in agreement with Fig. 1. Figure 2(a) exhibits the evolution of Hall resistance with the magnetic field at different temperatures. A critical magnetic field ($H_{\rm SW}$) for magnetization reversal could be defined as the equivalent magnetic field when the magnetic moment from the "up (down)" parallel state to the "down (up)" parallel state, which is related to the coercivity of magnetization reversal. Figure 2(b) presents the relationship between $H_{\rm SW}$ and T. It can be seen that $H_{\rm SW}$ gradually increases from 425 Oe to 3154 Oe with decreasing the temperature, in agreement with the feature of magnetic anisotropy enhancement when the temperature decreases, and the reverse magnetic domain nucleation position and the rate of domain wall motion also change significantly with decreasing temperature.[21]

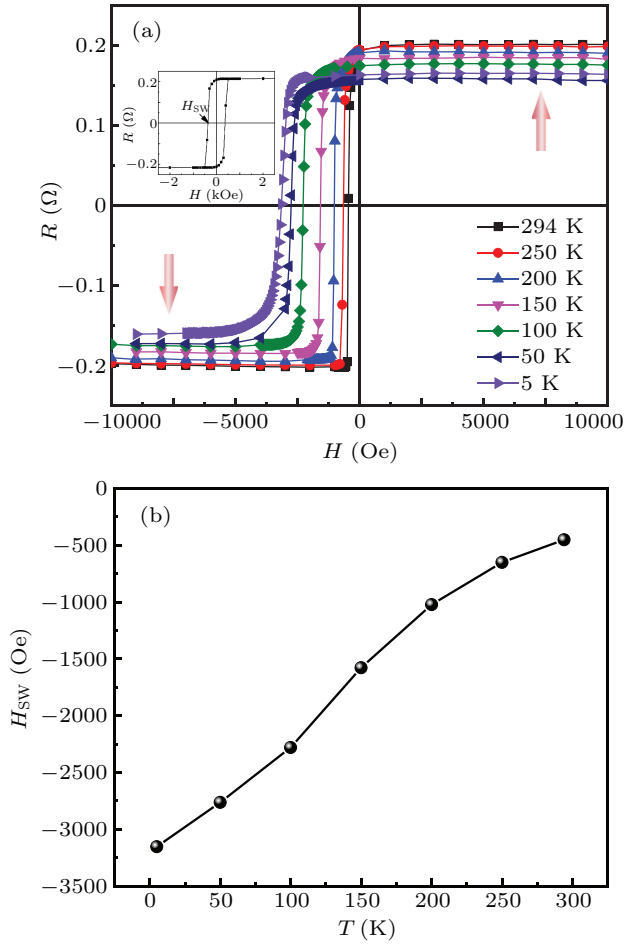


Fig. 2. The Hall resistance measurements: (a) Hall resistance curves measured at different temperatures, with inset showing the Hall resistance loop under 1 mA current; (b) the dependence of critical magnetic field on the temperature.

Regarding the analyses of the hybrid-driven magnetization reversal, an in-plane direct-current (DC) is applied with

an out-of-plane magnetic field as shown in the schematic diagram of Fig. 3(a), and the magnetization reversal was jointly driven by the applied magnetic field and current-induced SOT. The effective SOT field ($\Delta \boldsymbol{H}_{\rm DL}$) can be defined as[22]

$$\Delta \boldsymbol{H}_{\rm DL} = \hbar \theta_{\rm SH} J_{\rm e} / 2|e| M_{\rm s} t_{\rm FM} (\boldsymbol{\sigma} \times \boldsymbol{m}). \quad (1)$$

Here, $\boldsymbol{m}$ and $\boldsymbol{\sigma}$ are the unit vectors of the magnetic moment ($\boldsymbol{M}$) and the spin vector, $\hbar$ is the Planck constant, $\theta_{\rm SH}$ is the spin Hall angle, $J_{\rm e}$ is the density of the charge current flow, e is the amount of electron charge, $t_{\rm FM}$ and $M_{\rm s}$ are the thickness of the ferromagnetic layer and saturation magnetization. As shown in Fig. 3(a), the current-induced $\Delta \boldsymbol{H}_{\rm DL}$ can be decomposed into a perpendicular component ($\Delta \boldsymbol{H}^{x}_{\rm DL}$) and a parallel component ($\Delta \boldsymbol{H}^{z}_{\rm DL}$), where the $\Delta \boldsymbol{H}^{x}_{\rm DL}$ can cause the rotation of the magnetic moment $\boldsymbol{M}$ to move away from the z-axis, and the $\Delta \boldsymbol{H}^{z}_{\rm DL}$ is like an equivalent magnetic field to drive the magnetic moment reversal. The magnitude of the current-induced $\Delta \boldsymbol{H}_{\rm DL}$ will be increased with $J_{\rm e}$, so do $\Delta \boldsymbol{H}^{x}_{\rm DL}$ and $\Delta \boldsymbol{H}^{z}_{\rm DL}$. That is why the magnetization can be fully reversed with increasing the in-plane current, as presented in Fig. 3(b).

Figure 3(b) shows the $R_{\rm Hall}$–H_z curves of the Pd/CoZr/MgO thin films with different in-plane currents. It can be seen that the $H_{\rm SW}$ is reduced with the increment of current. As we know, the increment of current could generate a high spin current, resulting in a large SOT. Owing to the strong current-driven force, the magnetization can be reversed at a low magnetic field, showing a low $H_{\rm SW}$. It shows that the $H_{\rm SW}$ was reduced from 347 Oe to 248 Oe while the current increased from 7 mA to 20 mA, corresponding to the current density from 4.9×10^4 A/cm^2 to 1.4×10^5 A/cm^2.

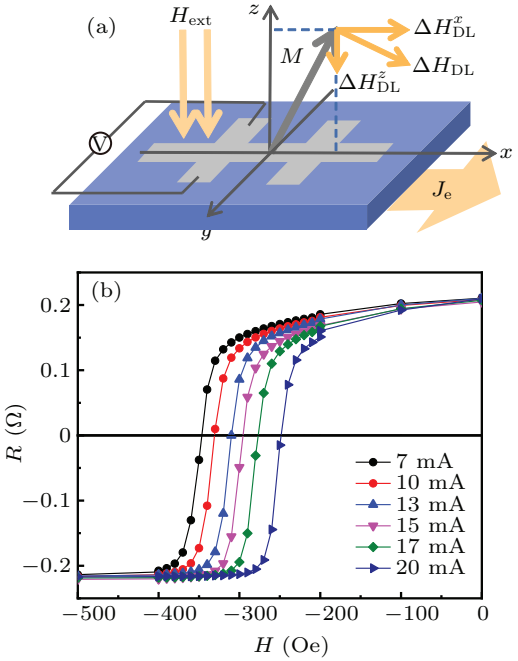


Fig. 3. The Hall resistance measurements: (a) the schematic diagram of the hybrid driven mode; (b) Hall resistance curves measured with different currents at 294 K.

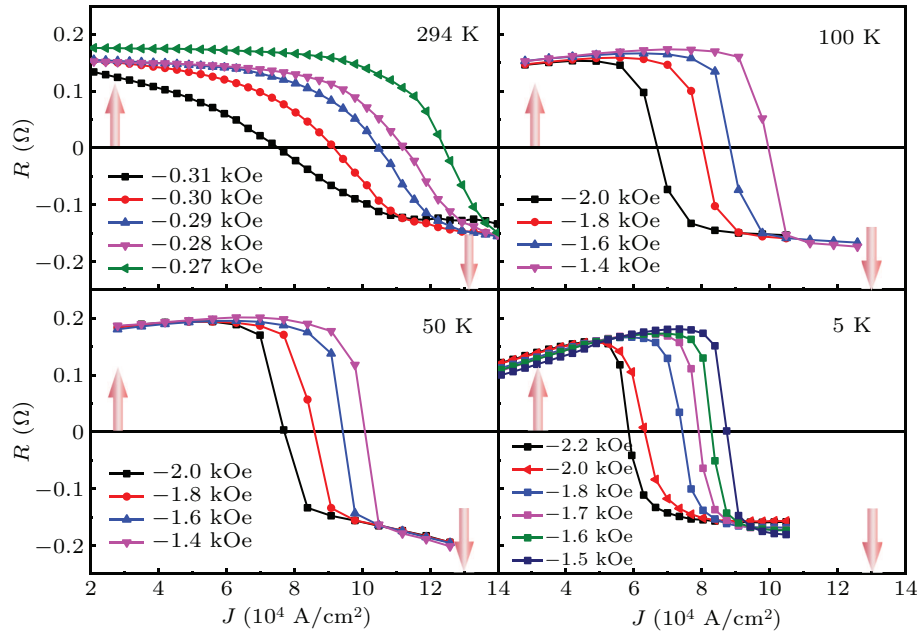


Fig. 4. The Hall resistance evolutions with the current density (R–J curves) at different temperatures.

As shown in Fig. 3, the magnetization reversal is highly related to the electric current. Therefore, we further investigated the behavior of the current-driven magnetic moment reversal at different temperatures. The measurement procedure is as follows: firstly, a large positive magnetic field of 5 kOe is applied to reach a positive saturation state, and then the Hall resistance is measured from 0.01 mA to 20 mA under an opposite magnetic field, which is slightly less than $H_{\rm SW}$, in which the sweeping rate of current is 0.125 mA/s. Figure 4 presents the relationships of Hall resistance with the current at differ-

ent temperatures under a varied magnetic field. It shows that the Hall resistance slowly decreases from the positive maximum value as the current increases and tends to the negative maximum value, indicating that magnetization could be fully reversed under a critical current. The critical current density is in the order of 10^4–10^5 A/cm^2, which is much lower than the value of pure current-driven reversal. It exhibits that the critical current is highly relevant to the applied magnetic field and temperature.

Regarding the magnetization reversal at a certain temperature, the insufficiency of driving force under the magnetic field will be compensated through the current-induced SOT, or vice versa. Thus, we could evaluate the equivalent correlation between the magnetic field and the current-induced SOT, as shown in Fig. 5. It is obvious that the equivalent correlation is dependent on the temperature. There exists an increasing tendency of equivalent current density for a certain magnetic field except the equivalent correlation at the measuring temperature of 5 K. One example was taken as shown in Fig. 5, the equivalent current density (ΔJ) of 200 Oe (ΔH) increases with temperature except the temperature of 50 K. As we know, the current-induced SOT is proportional to the spin current. The spin current generated by heavy metals can be evaluated according to the formula

$$\boldsymbol{J}_\mathrm{s} = (\hbar/2e)\,\theta_\mathrm{SH}\boldsymbol{\sigma} \times \boldsymbol{J}_\mathrm{e}, \tag{2}$$

where $\boldsymbol{J}_\mathrm{s}$ is the spin current density; it can be seen that the generation of spin current is also related to the spin vector $\boldsymbol{\sigma}$ and the spin Hall angle θ_SH. Generally, the spin vector decreases with increasing temperature. It is reported that the θ_SH presents a parabolic variation with temperature, showing a turning point of around 50 K.[23] These mean that the $\boldsymbol{J}_\mathrm{s}$ generated from the $\boldsymbol{J}_\mathrm{e}$ shows increasing tendency with increasing temperature in the range below 50 K and decreasing tendency in the range above 50 K. This is why the equivalent correlation is different at the temperature of 5 K. It is well known that the magnetic anisotropy of film will be weakened with increasing temperature, indicating that the magnetization reversal becomes easier.

The decreases of $\theta_\mathrm{SH}$and $\boldsymbol{\sigma}$ would weaken the conversion of $\boldsymbol{J}_\mathrm{e}$ to $\boldsymbol{J}_\mathrm{s}$ at the higher temperature, indicating that the current-induced equivalent magnetic field could be weakened too. The θ_SH decreases with the decrease of temperature in the range below 50 K; the SOT generated by the current could have the same trend. Therefore, a larger current is needed to drive the magnetization reversal with a fixed magnetic field. Interestingly, Fig. 5 may show that the current-driven magnetization reversal will be more efficient at a low temperature since the force originated from SOT is equivalent to a high magnetic field; and applying magnetic field will be helpful for magnetization reversal in a high temperature range because a low magnetic field need be compensated for by a large current density.

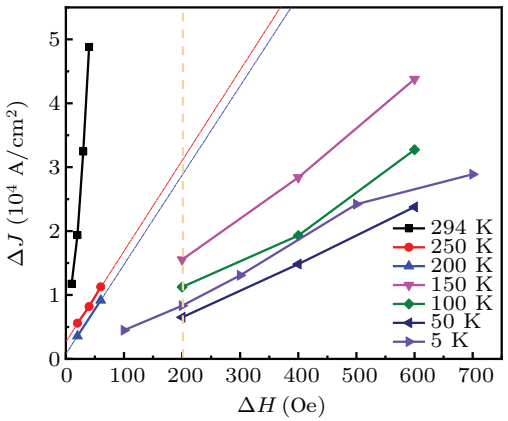


Fig. 5. The equivalent correlation between the increments of the switching current and the magnetic field at different temperatures.

4. Conclusions

The large PMA has been realized in Pd/CoZr/MgO trilayer films with a relatively thick ferromagnetic layer, which is favorable for achieving a low Gilbert damping coefficient. Inspired by the hybrid electric car and heat-assisted magnetic recording, we have demonstrated a hybrid driven mode of magnetization reversal for Pd/CoZr/MgO perpendicular magnetic films, the joint driving reversal through the current-induced spin-orbital torque and magnetic field at different temperatures. The critical current density of magnetization reversal can be reduced to the magnitude of 10^4–10^5 A/cm^2 with the hybrid driving way, which is much lower than the common value of $> 10^6$ A/cm^2 of pure current-driven mode. The equivalent correlation between the current-induced torque and magnetic field is evaluated, which exhibits an obvious dependence on the temperature. It is found that the current-driven magnetization reversal will be more efficient at low temperature, and magnetic field will be helpful for magnetic reversal in high temperature range.

Acknowledgements

This work was supported by the ISF-NSFC Joint Research Project of International Cooperation and Exchanges (Grant No. 51961145305), the National Natural Science Foundation of China (Grant Nos. 52171191 and 51771145), the Shaanxi Key Program for International Science and Technology Cooperation Projects (Grant No. 2021KWZ-12), and the Youth Innovation Team of Shaanxi Universities.

References

[1] Berger L 1996 *Phys. Rev. B* **54** 9353
[2] Slonczewski J C 1996 *J. Magn. Magn. Mater.* **159** L1
[3] Xue J, Guo Y, Wang L, Dong Y and Bai L 2019 *J. Magn. Magn. Mater.* **496** 165932
[4] Manchon A, Zelezny J, Miron I M, Jungwirth T, Sinova J, Thiaville A, Garello K and Gambardella P 2018 *Rev. Mod. Phys.* **91** 035004

[5] Yun J J, Li D, Cui B, Guo X, Wu K, Zhang X, Wang Y, Zuo Y and Xi L 2017 *J. Phys. D: Appl. Phys.* **50** 395001
[6] Zhu L, Ralph D C and Buhrman R A 2019 *Phys. Rev. Lett.* **122** 077201
[7] He C L, Chen Q Q, Shen S P, Wei J W, Xu H J, Zhao Y C, Yu G Q and Wang S G 2021 *Chin. Phys. B* **30** 037503
[8] Zhu L, Ralph D C and Buhrman R A 2021 *Appl. Phys. Rev.* **8** 031308
[9] Bai Q W, Guo B, Yin Q and Wang S Y 2022 *Chin. Phys. B* **31** 017501
[10] Liu L, Pai C F, Li Y, Tseng H W, Ralph D C and Buhrman R A 2012 *Science* **336** 555
[11] Liu L, Lee O J, Gudmundsen T J, Ralph D C and Buhrman R A 2012 *Phys. Rev. Lett.* **109** 096602
[12] Yang H X, Chshiev M, Dieny B, Lee J H, Manchon A and Shin K H 2011 *Phys. Rev. B* **84** 054401
[13] Zhang W, Valloppilly S R, Li X, Skomski R, Shield J E and Sellmyer D J 2012 *IEEE Trans. Magn.* **48** 3603
[14] Christopher N, Anand K and Singh N 2021 *Solid State Commun.* **323** 114118
[15] Motalebi E, Tavoosi M, Ghasemi A, Gordani G R, Torkian S and Loghman-Estarki M R 2019 *Appl. Phys. A* **125** 502
[16] Li C Z, Jiang C J and Chai G Z 2021 *Chin. Phys. B* **30** 037502
[17] Lin W W, Sang H, Liu D, Jiang Z S, Hu A and Wu X S 2006 *J. Appl. Phys.* **99** 08G518
[18] Xie K X, Lin W W, Sun H C, Nie Y and Sang H 2008 *J. Appl. Phys.* **104** 083907
[19] Oh Y W, Lee K D, Jeong J R and Park B G 2014 *J. Appl. Phys.* **115** 17C724
[20] Liu Y, Yuan Z, Wesselink R J H, Starikov A A and Kelly P J 2014 *Phys. Rev. Lett.* **113** 207202
[21] Zhu J R, Fan L C, Su Y C and Hu J G 2016 *Acta Phys. Sin.* **65** 237501 (in Chinese)
[22] Yu G, Upadhyaya P, Fan Y, Alzate J G, Jiang W, Wong K L, Takei S, Bender S A, Lang M and Tang J 2014 *Nat. Nanotechnol.* **9** 548
[23] Ma L, Lang L, Kim J, Yuan Z, Wu R, Zhou S and Qiu X 2018 *Phys. Rev. B* **98** 224424